

pubs.acs.org/JPCB Article

Carbon Nanoparticle-Induced Changes to Lipid Monolayer Structure at Water—Air Interfaces

Nida Shaikh, Jessica M. Andriolo, Jack L. Skinner, and Robert A. Walker*



Cite This: J. Phys. Chem. B 2022, 126, 5667-5677



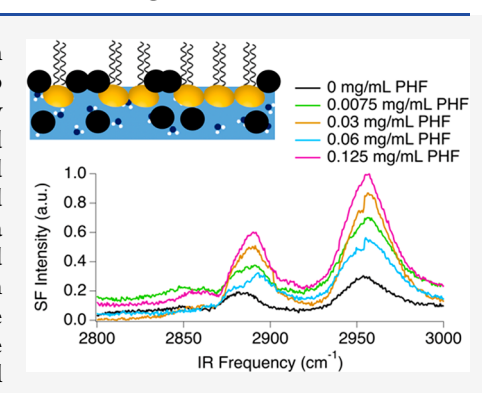
ACCESS

III Metrics & More

Article Recommendations

SI Supporting Information

ABSTRACT: Surface specific vibrational spectroscopy experiments together with surface tension measurements and spectroscopic ellipsometry data were used to characterize the effects of soluble carbon particulates on compressed and partially compressed lipid monolayers adsorbed to the water—air interface. The lipid monolayers consisted of 1,2-dimyristoyl-sn-glycero-3-phosphocholine (DPPC), and measurements were made for both tightly packed monolayers (40 Ų/molecule) and monolayers in their liquid condensed state (55 Ų/molecule). Langmuir trough data show that very small amounts of PHF (0.0075 mg/mL or 6.4×10^{-6} M) decrease lipid film compressibility. This finding supports a cooperative adsorption mechanism whereby the soluble PHFs are drawn to the surface and associate with the insoluble DPPC monolayer. Excess free energies ($\Delta G_{\rm mix}^{\rm E}$) were positive, consistent with the cooperative adsorption mechanism, and although the excess free energies are small (≤ 1 kJ/mol), adsorbed PHF has measurable effects on monolayer structure. Further



support for the cooperative adsorption mechanism at the water—air interface comes from vibrational sum frequency generation (VSFG) experiments. Low PHF concentrations (\leq 0.06 mg/mL) increase DPPC acyl chain ordering in liquid condensed lipid films and decrease DPPC acyl chain ordering and film thickness in tightly packed lipid films.

■ INTRODUCTION

Agencies that monitor air pollution (i.e., EPA and FAA) recognize black carbon (BC) as a component of PM_{2.5} (particulate matter <2.5 μ m in diameter) produced by both natural and anthropogenic combustion processes such as open biomass burning and transportation. Because BC is the product of incomplete combustion, it is a heterogeneous material consisting of correspondingly diverse behaviors. In this context, BC is a fundamentally different material than the more traditional carbon black (CB)—a fine black powder of nearly pure elemental carbon manufactured intentionally for use in products ranging from automobile tires to paint. BC aerosol adsorption to biologically relevant water—air interfaces such as alveoli surfaces has long been associated with health risks and is linked to increased mortality rates throughout the world.²⁻⁴ Specific to pulmonary diseases, BC aerosols change the structural, elastic, and dynamic properties of lung surfactant. 5,6 The mechanisms responsible for these effects, however, remain under debate. Specifically, the impact of carbon particulates on lung surfactant structure and organization and the consequences of these interactions on lung surfactant's dynamic properties remain correlative at best. Furthermore, the chemistry of these heterogeneous systems becomes even more complex when one considers that BC itself changes as a function of time. While BC typically starts out hydrophobic with high carbon content, oxidative processes render aged BC much more hydrophilic and highly soluble in aqueous solution.7-

Previous studies have found that BC particulates age in the atmosphere through condensation and coagulation processes. 12 More recent studies have found that freshly generated BC becomes coated by water-soluble material during atmospheric aging, including condensation of sulfate, nitrate, and small volatile organic species, coagulation with preexisting aerosols, and heterogeneous reactions with gaseous oxidants. Consequently, BC aerosols transform from having a surface of primarily carbon and being strongly hydrophobic to having oxygenated functional groups that make the surface more hydrophilic.¹³ Models exist to estimate BC aging time, but predictions from these models are inconsistent. For example, in one model the average BC aging rate in Beijing, China, is predicted to be roughly 7 times faster than that in Houston, TX. In another model ~23 h on average is required in Beijing, China, to complete the hydrophobic-to-hydrophilic conversion, while it takes ~8 h for the same conversion process to occur in Houston, TX.14 Regardless of the models being used and the variable BC aging rates, the aging process for BC, specifically the hydrophobic-to-hydrophilic conversion process,

Recived: April 12, 2022 Revised: July 12, 2022 Published: July 25, 2022





happens on a very short time scale considering the lifetime of BC in aerosols ranges from days to weeks. Given this variable evolution of BC properties, one might reasonably expect the physiological impact of BC aerosols on lung surfactant function to also change over time.

Studying the effects of BC on lung surfactant typically proceeds in one of two ways. At a physiological scale, in vitro and in vivo experimental systems correlate the effects of carbonaceous pollutants by directly linking inhalation of and exposure to nonbiological particulates in the atmosphere/ environment to cardiorespiratory health impacts, including susceptibility to respiratory viruses, particle-induced lung cancer, pulmonary pathophysiologic changes, and cardiac injury. 15-18 For example, the FAA uses a combination of field monitoring and dispersion modeling studies along with statistical methods to estimate BC aerosol toxicity. Additionally, EPA researchers have developed models such as the human exposure model (HEM) to perform risk assessments from sources that emit toxic aerosols into ambient air (i.e., studying the inhalation pathway of exposure to make predictions about risks associated with toxic aerosols). EPA models such as the HEM are also being used to further learn about BC composition, compare BC impacts relative to those of other airborne particles, evaluate how particulates absorb and scatter different wavelengths of light, and study the effects of BC on human health through controlled clinical studies examining effects from exposure to different air quality. Very few of these studies investigate fundamental interactions between BC and lung surfactant at the molecular level. 19,20

A second approach attempts to identify specific particulate surfactant interactions by distilling the system's complexity to its component parts, starting from the level of model systems to generalize to larger, ensemble effects. S,21,22 On the basis of *in vitro* and *in vivo* studies, particular concern are the class of particles labeled PM_{2.5} (<2.5 μ m in diameter) and especially particles smaller than 100 nm as they can be readily inhaled and penetrate deep into the lungs and bloodstream and translocate to other organs and tissues. Both approaches—physiological and model system studies—are necessary. The physiological studies identify the impact of BC on lung surfactant function, and the laboratory, model-system experiments provide the detailed, molecular level insight necessary for developing predictive models.

This work is inspired by in vivo reports suggesting that insoluble elemental carbon nanoparticles, models for freshly generated BC with high elemental carbon content, within a 1,2-Dimyristoyl-sn-glycero-3-phosphocholine (DPPC) monolayer affect DPPC domain growth by inducing DPPC, a model for lung surfactant, to first form incompressible microscopic domains that exclude the nanoparticles.^{2,21} The domains then increase in size as more DPPC molecules adhere to the domain perimeter. Because the carbon nanoparticles aggregate around the lipid domain perimeters, smaller domains are unable to come together and form larger structures, leading to reduced monolayer elasticity and decreased rigidity.² While this scenario may accurately capture the interactions between lipid monolayers—and, by extension, lung surfactant—and hydrophobic carbon particulates, findings may not be as relevant to lipid monolayer-hydrophilic carbon particulates such as those that have become oxidized in the atmosphere upon aging.

Work described in this article uses optical and thermodynamic methods to evaluate the effects of soluble carbon

particulates, chosen as models for aged BC, on DPPC monolayers adsorbed to the water-air interface as a function of monolayer compression. The model system used in this work was chosen to reproduce many of the features found at the tissue-air interface in lungs. Lung alveoli consist of a water-air interface covered with a surfactant mixture composed of lipids (90% by mole fraction), cholesterol (10%), and trace amounts of SP proteins.²³ This surfactant mixture reduces water-air interfacial tension and enables alveoli to expand and contract during respiration with significantly reduced mechanical effort.^{24–27} Lung surfactant also represents the final line of defense against aerosol inhalation⁵ and serves as a barrier that prevents inhaled particulates from entering the bloodstream and translocating to other organs. In the context of this article, there are two components comprising the model system being used to carry out experiments: (1) lung surfactant and (2) black carbon. Because DPPC is the majority component of lung surfactant, DPPC monolayers adsorbed to aqueous-air interfaces are commonly used to model lung surfactant surface properties such as fluidity, permeability, and miscibility (in mixed Langmuir films). ^{24,28–30} Because freshly generated BC aerosols generally start out with high elemental carbon content and are quite hydrophobic,³¹ but as they age and become oxidized their elemental carbon content decreases, making them hydrophilic and water-soluble, 9-11 soluble carbon nanoparticles are often used to model aged BC. Polyhydroxylated fullerenes (PHFs), also known as "fullerols" or "fullerenols", comprise a family of soluble carbon particulates (CPs) with solubilities as high as 58.9 g/L in water, 7,8 making them reasonable surrogates for aged BC aerosols.^{32–34}

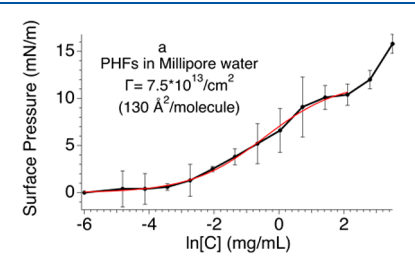
In the studies described below, surface tension measurements, surface-specific vibrational sum frequency generation (VSFG) spectroscopy, and spectroscopic ellipsometry (SE) are used to examine the effects of PHFs on DPPC Langmuir monolayer structure and organization. Measurements are performed at two DPPC monolayer surface coverages: 55 Å²/molecule (corresponding to a monolayer in its liquid condensed state) and 40 Å²/molecule (corresponding to a tightly packed DPPC monolayer). Findings show that inappreciable amounts of PHF in solution directly impact monolayer organization. This result is significant by itself given that with PHF high bulk solubility simple equilibrium considerations would predict that PHF concentrations below ≤0.125 mg/mL should lead to vanishingly small surface excess concentrations with very little impact on DPPC monolayer structure. Given that low PHF concentrations do affect DPPC monolayer structure strongly suggests a cooperative adsorption model where the DPPC attracts and retains PHFs in the surface/near-surface region, enriching the interface's organic content and forcing the DPPC monomers to adopt a more ordered structure.

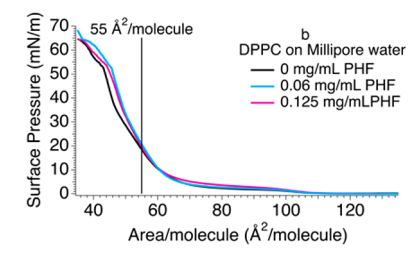
METHODS

Materials. 1,2-Dimyristoyl-sn-glycero-3-phosphocholine (DPPC) was purchased from Avanti Polar Lipids Inc. (powder, >99% purity; Alabaster, AL) and used as received. PHFs were purchased from American Elements (Los Angeles, CA) and used as received. The PHFs themselves consisted of a mixture of species having the general formula $C_{60}(OH)_n \cdot mH_2O$, where $n = 22 \pm 2$ (determined by SEC-HPLC) and m > 8. HPLC-grade chloroform, used as the DPPC spreading solvent, was purchased from Fisher Scientific (99.9% purity; Waltham,

MA). The aqueous subphase used was water from a Millipore filtration system (Synergy by Millipore). Before any addition of lipids or PHFs, the subphase had a resistivity of 18.2 M Ω and a surface tension of 72.5 mN/m at 23 °C.

Sample Preparation. Sample preparation has been described previously.^{24,35,36} Millipore water was used for all aqueous sample preparations. Polyhydroxylated fullerene stock solutions (0.5 mg/mL) were prepared in Millipore water and sonicated for 5 min. The polyhydroxylated fullerene stock solutions were used to prepare aqueous PHF mixtures of 0.0075, 0.03, 0.06, 0.125, and 0.5 mg/mL. DPPC lipid stock solutions (~0.4-0.7 mg/mL) were prepared in chloroform and sonicated for 10 min. Aqueous PHF samples for VSFG measurements were prepared in borosilicate Petri dishes. The Petri dishes were rinsed with methanol, acetone, and Millipore water several times prior to acid washing (50/50 vol nitric/ sulfuric) and then rinsed with Millipore water several times after acid washing and before use. Surface tension measurements of these systems show PHFs to be very weakly surface active with surface concentrations of $7.5 \times 10^{13}/\text{cm}^2$ at the highest bulk concentrations used in these studies (see Figure 1a and Table S1). For all Langmuir trough, VSFG, and SE experiments, a Hamilton glass microsyringe was used to apply the appropriate amount of the DPPC/chloroform stock





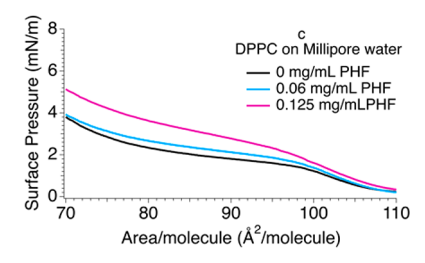


Figure 1. (a, top) Surface tension measurements ($\ln[C]$ vs surface pressure) demonstrating surface activity by employing Gibbs adsorption equation, where [C] is PHF concentration. The red line is an empirical fit of the data to a sigmoidal function and is used to calculate slope at different bulk solution PHF concentrations. All data reported in (a) are the average of 3–6 measurements taken for each PHF concentration. (b, middle) Langmuir trough compression isotherms of DPPC with PHF subphase of varying concentrations. (c, bottom). An expanded view of Langmuir trough compression isotherm data showing slight, systematic shifts in liftoff and slope with changing PHF concentrations.

solution to the aqueous subphase surface to ensure the desired surface coverage of 55 or 40 Ų/molecule with an uncertainty of ± 3 Ų/molecule. After the DPPC was deposited at the water—air interface, the sample was allowed to sit for ≥ 5 min so that the chloroform could evaporate and the DPPC monolayer could equilibrate—DPPC was deposited on both a neat Millipore subphase and aqueous PHF subphases of varying PHF concentrations.

Surface Tension and Langmuir Trough. Surface tension measurements and Langmuir trough compression isotherms were obtained by using methods described previously. ^{24,35,36} Simple surface tension measurements were performed to quantify PHF surface activity. These experiments consisted of preparing Millipore solutions having different PHF concentrations, measuring the surface tension with a calibrated, NIMA PS-4 pressure sensor (with a paper Wilhelmy plate), and converting the surface tension to surface pressure (eq 1):

$$\Pi = \gamma_0 - \gamma \tag{1}$$

In experiments designed to determine whether or not the soluble PHFs are surface-active, surface pressure is plotted as a function of the natural log of concentration, and surface excess concentrations are determined by using the Gibbs isotherm equation (eq 2a).³⁷ All surface tension data reported are the average of 2–6 measurements taken for each PHF concentration.

$$\Pi A = nk_{\rm B}T \ln(c) \tag{2a}$$

$$\Gamma = \frac{n}{A} = \frac{1}{k_{\rm B}T} \frac{\mathrm{d}\Pi}{\mathrm{d}\ln c} \tag{2b}$$

In eqs 2a and 2b, Γ is the surface excess concentration, A is the sample area, n is the number of adsorbed species, $k_{\rm B}$ is Boltzmann's constant, T is temperature (in K), and c is the PHF concentration. Note that for the experiments described here a 1 mg/mL PHF solution was chosen as a reference concentration which corresponds to \sim 0.8 mM. Terminal surface coverage is determined from the slope of steepest ascent (eq 2b).

To assess the effects of soluble PHFs on insoluble DPPC monolayers, compression isotherms were acquired by using a NIMA Langmuir trough (model 302LL) equipped with a NIMA PS-4 pressure sensor and a microprocessor interface. To obtain Langmuir trough compression isotherms, Langmuir trough barriers were closed at a speed of 12 cm²/min, although slowing this compression by a factor of 3 did not change observed results. Surface pressure (Π) was measured as a function of surface area.

Given that the PHFs were found to be only weakly surface active, we can calculate excess free energies of mixing, $\Delta G_{\text{mix}}^{\text{E}}$, as illustrated in eq 3. In eq 3, A_{12} is the actual area per molecule of a mixed monolayer, A_1 and A_2 are the area per molecule of a pure monolayer of one of the species in the mixed monolayer, and x_1 and x_2 are the mole fractions of each of the species in the mixed monolayer.

$$\Delta G_{\text{mix}}^{\text{E}} = \int_{\pi_1}^{\pi_2} N_A (A_{12} - x_1 A_1 - x_2 A_2) \, d\pi$$
(3)

Equation 3 can be further simplified. Because PHFs are highly soluble in aqueous solution (>50 mg/mL in H_2O), we assume that DPPC (species 1) is the only species constrained to the

water—air interface. Using this assumption, eq 3 simplifies to eq 4.

$$\Delta G_{\text{mix}}^{\text{E}} = \int_{\pi_1}^{\pi_2} N_A (A_{12} - A_1) \, d\pi$$
 (4)

Therefore, by integrating the differences in area between the isotherm from the system of interest and that of pure DPPC as a function of surface pressure, the excess free energy of mixing can be determined. We note here that if the PHFs showed no affinity for the DPPC monolayer, this integral would equal zero.

Vibrational Sum Frequency Generation Spectroscopy. Vibrational sum frequency generation (VSFG) is a second-order nonlinear spectroscopy technique that has been described in detail previously. 24,35,36,40,41 Interfaces break the inversion symmetry between centrosymmetric media, leading to VSFG becoming symmetry allowed provided that species at the interface have a net polar ordering. 42 To perform VSFG experiments, two oscillating electromagnetic fields at different frequencies (fixed visible 800 nm and a tunable IR) are overlapped both spatially and temporally on a surface of interest. The two fields couple through the second-order susceptibility tensor, $\chi^{(2)}$, and create a coherent nonlinear polarization equal in frequency to the sum of the two input frequencies.

In SFG experiments, the intensity of the resultant SF signal, $I(\omega)$, is proportional to the square of the effective portion of the second order nonlinear susceptibility, $\chi_{\rm eff}^{(2)}$, as shown in eq 5. The $\chi_{\rm eff}^{(2)}$ consists of two parts: a resonant contribution $(\chi_{\rm q,eff}^{(2)})$ and a nonresonant contribution $(\chi_{\rm NR,eff}^{(2)})$, as shown in eq 6. When the IR frequency $(\omega_{\rm IR})$ is resonant with a vibrational mode $(\omega_{\rm q})$ of surface species, the SF signal generated is resonantly enhanced, as displayed in eq 6.

$$I(\omega) \propto |\chi_{\text{eff}}^{(2)}|^2$$
 (5)

$$|\chi_{\text{eff}}^{(2)}|^2 = \left|\chi_{\text{NR,eff}}^{(2)} + \sum \frac{\chi_{\text{q,eff}}^{(2)}}{\omega_{\text{IR}} - \omega_{\text{q}} + i\Gamma_{\text{q}}}\right|$$
 (6)

Reported VSFG spectra were acquired under SSP polarization conditions (listed in order of sum, visible, and IR polarizations, respectively: $S_{\text{sum}}S_{\text{vis}}P_{\text{IR}}$). The SSP polarization combination samples a single $\chi^{(2)}$ element, $\chi^{(2)}_{iiz}$, and is sensitive to only those vibrations whose IR transition moment is aligned along the surface normal (assigned as the *z*-axis). r^+/d^+ ratios reported from VSFG spectra are the average of 2–5 measurements taken per sample.

The VSFG setup used has been described in detail elsewhere. 24,35,36 Briefly, ~ 3.4 W from a Ti:sapphire regenerative amplifier (Libra-HE, Coherent, 85 fs pulses, 1 kHz repetition rate, 800 nm) was coupled to an optical parametric amplifier (Coherent OPerA Solo). An 80/20 beam splitter reflects 80% of the 800 nm into a tunable Coherent OPerA Solo optical parametric amplifier to produce IR light. The 800 nm light and the IR light (centered at $\sim 3.4~\mu m$) are then aligned both spatially and temporally and then focused onto the sample of interest at 48° and 38°, respectively, from surface normal. The SF response is then collimated and isolated before being focused into a monochromator (SpectraPro-300i, Action Research Corporation). The SF response is then dispersed into a 1340 \times 100 pixel CCD (PIXIS100B, Princeton Instruments).

Spectra reported in this work measure the s-polarized SFG response arising from s-polarized visible and p-polarized IR fields (SSP). This polarization combination measures a single element of the $\chi^{(2)}$ tensor ($\chi^{(2)}_{xxz}$). Under this condition, the relative intensities of the methyl symmetric stretch (r+) and methylene symmetric stretch (d⁺) are significant. Highly ordered DPPC films with acyl chains in all-trans conformations will have methyl groups organized with their local $C_{3\nu}$ axes aligned approximately along the surface normal (designated as the z direction in the laboratory frame of reference) and the local $C_{3\nu}$ axes of the methylene groups aligned in the x-yplane, parallel to the water surface. A consequence of this structure is that an SFG spectrum will have an intense r⁺ signature and a very weak d+ response. Furthermore, acyl chains in an all-trans conformation will have local inversion symmetry about the center of each carbon-carbon bond making d⁺ symmetry forbidden due to IR and Raman mutual exclusivity in centrosymmetric systems. Introduction of overall monolayer tilt and/or gauche defects in the chain will increase d^+ intensity and diminish r^+ intensity. As a result, a large r^+/d^+ ratio is expected from a well-ordered monolayer with acyl chains aligned along the surface normal and having very few gauche defects. Conformational disorder and/or disordered chains will result in a VSFG spectrum having a smaller r⁺/d⁺ ratio. Tightly packed, saturated, phosphocholine monolayers at the aqueous-air interface typically have r+/d+ ratios in excess of 5. 23,24,27,34 The reported uncertainty in r^+/d^+ ratios from VSFG spectra represents the standard deviation from 3 to 6 independent experiments/spectra. We speculate that some of the observed variability may be due to concentrationdependent sensitivity in the distribution between PHF monomers versus aggregates in bulk solution.

Spectroscopic Ellipsometry. Spectroscopic ellipsometry experiments were performed with a J.A. Woollam RC-2, and data were analyzed in CompleteEASE, a modeling software application distributed by J.A. Woollam. The beam from the instrument was calibrated in the source and detector prior to every measurement. The signal detected was the change in polarization upon the incident beam irradiating the sample, which was quantified through ellipsometric angles Ψ (amplitude ratio) and Δ (phase difference) in eqs 7 and 8, respectively.

$$\tan(\Psi) = \frac{|R_p|}{|R_s|} \tag{7}$$

$$\Delta = \Delta_{p} - \Delta_{s} \tag{8}$$

$$\rho = \frac{R_{\rm p}}{R_{\rm s}} = \tan(\Psi)e^{i\Delta} \tag{9}$$

A sample of pure Millipore water matched with a mean standard error (MSE) of 0.99–2.28 at the start of the measurements to a model of water at 25 °C. The incident angle was set at 75° with the thickness set to fit. Once Ψ and Δ were obtained, the complex reflectance ratio (ρ) was determined by using eq 9 and then used to derive the optical constants (i.e., film thickness) of lipid films at the air—water interface. Specifically, SE was used to monitor changes to DPPC monolayer thickness with the inclusion of PHFs to both 55 and 40 Ų/molecule deposited DPPC. Monolayer thicknesses reported from SE experiments are the average of six measurements taken per sample. The SE model used for

fitting assumes no PHFs are present—only DPPC is present at the surface. Knowing that the PHFs are weakly surface-active, we then use the "neat" DPPC model as a reference to assess how the addition of PHFs change DPPC monolayer thickness.

RESULTS

Surface Tension and Langmuir Trough. To address whether soluble PHFs affect insoluble DPPC monolayer structure and organization, experiments were first performed to determine if the PHFs themselves were surface-active. Surface tension measurements of PHF-containing aqueous solutions were measurements as a function of PHF concentration, and results were plotted as surface pressure (P) versus the natural log of PHF concentration (Figure 1a). The rise in surface pressure as a function of PHF concentration in Figure 1a shows that these soluble solutes are in fact surfaceactive, and the isotherm itself shows unusual behavior. After passing through an inflection point at a concentration of ~0.37 mg/mL (ln[C] = -1.0) and starting to plateau, the surface pressure starts to rise steeply again at PHF concentration above $\sim 7.4 \text{ mg/mL} (\ln [C] > 2.0)$. Vibrational spectroscopy and ellipsometry experiments show that PHF effects on lipid monolayer organization are most pronounced in the low PHF concentration limit, so all further results described below are performed with solutions having PHF concentrations < 0.125 mg/mL (= <-2.8 in Figure 1a). PHF surface behavior at higher concentrations will be the subject of future studies.

Analyzing the data in Figure 1a by using the Gibbs adsorption equation (eqs 2a and 2b) leads to a terminal monolayer coverage of 7.5×10^{13} cm⁻² or, equivalently, $\sim \! 130$ Ų/molecule. Given an estimated PHF radius of $\sim \! 4.5$ Å, each PHF has a 64 Ų footprint, meaning that PHFs adsorbed to the aqueous—air interface are not tightly packed. As the VSFG and SE experiments described below will show, most of the changes induced by PHFs on DPPC monolayer organization occur at PHF concentrations below 0.06 mg/mL where PHF surface coverage (at the neat water—air interface) is even smaller $(2.6 \times 10^{13} \ \text{cm}^{-2} \ \text{or} \ 380 \ \text{Å}^2/\text{molecule})$.

DPPC compression isotherms were acquired on a Langmuir trough having different amounts of PHF present in the subphase (Figure 1b). The pure DPPC isotherm lifts off at (\sim 100 Å²/molecule) and passes through a liquid expandedliquid condensed coexistence region between 90 and 60 Å²/ molecule. The monolayer collapses with a terminal surface coverage of 42 $\text{Å}^2/\text{molecule}$, in agreement with previous reports. The isotherms show slight but measurable deviations with PHF subphase concentration. Specifically, increasing PHF concentration leads to slightly expanded monolayers where a given surface pressure corresponds to increasingly larger areas. In this context, areas are reported as areas per DPPC monomer given that PHFs are only weakly surface active with a coverage corresponding to $>200 \text{ Å}^2/$ molecule at the neat aqueous—air interface for a concentration of 0.125 mg/mL. As will be discussed below, we believe that the DPPC monolayer actually enriches PHF at the interface in ways that enhance lipid structure and organization.

Excess Free Energy of Mixing. Because adsorbed DPPC is constrained to the surface, integrating the differences in area between the isotherm from the system of interest and that of pure DPPC as a function of surface pressure provides information about mixing behavior at the interface. A positive $\Delta G^{\rm EX}$ value reflects a more expanded mixed monolayer relative to the weighted sums of the pure components. Similarly, a

negative ΔG^{EX} value implies that the mixed monolayer is more compressed with attractive interactions between the constituent components. Such an interpretation is misleading for the DPPC/PHF system. The isotherms in Figure 1b show that at a given surface pressure, the small amount of PHF in solution leads to a larger DPPC mean molecular area (MMA), but if PHFs are being drawn to the surface through cooperative interactions, then their adsorption from the bulk to the waterair interface will force the DPPC monomers to become more tightly packed. Similar results have been reported previously with soluble alkyl surfactants and with simple monosaccharides. 35,36,47 VSFG data below suggest that such a picture accurately describes the effects of PHFs on DPPC monolayers in the liquid condensed state (55 Å²/molecule). Langmuir trough compression isotherm data from Figure 1b were analyzed by using excess free energy expressions shown in eqs 3 and 4. $\Delta G^{\rm EX}$ values in Figure 2 show positive excess free

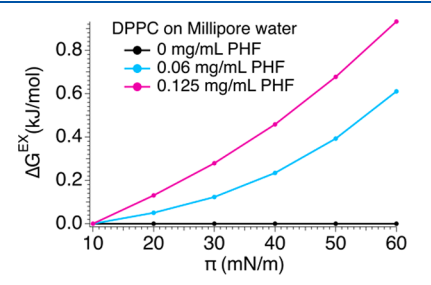


Figure 2. Excess free energy of mixing for DPPC with PHF subphase of varying concentration obtained from data in Figure 1b.

energies, consistent with PHF cooperative adsorption, and although the excess free energies are small, they have measurable effects on monolayer structure (*vide infra*).

While thermodynamic data are instructive, they do not provide information about molecular structure and organization. Discerning molecular structure and organization at interfaces is often challenging due to the small number of molecules involved and the sometimes large, overwhelming responses from bulk solution responses. To determine how inclusion of surface-active, soluble carbonaceous particulates changes lipid film structure and organization, VSFG was used to measure vibrational spectra of DPPC monolayers in their liquid condensed and tightly packed states.

VSFG (Spectra and r^+/d^+ Ratios). Figures 3a and 3b show VSFG spectra in the CH stretching region of DPPC monolayers in their liquid condensed and tightly packed states. Following convention, "r" denotes vibrations associated with the DPPC methyl group and "d" describes vibrations associated with methylene groups. 48,49 The "+" indicates a symmetric stretch (SS) and a "-" indicates an antisymmetric stretch (AS). d+ at 2850 cm-1 corresponds to a CH₂ SS, r+ at 2874 cm⁻¹ corresponds to a CH₃ SS, r⁻ at 2952 cm⁻¹ corresponds to an out-of-plane CH $_3$ AS, r^- at 2962 cm $^{-1}$ corresponds to an in-plane CH $_3$ AS, and r^+_{FR} at 2930 cm $^{-1}$ corresponds to a CH₃ Fermi resonance interaction. ^{24,50} Note that the *y*-axes report intensities in "arbitrary units" (a.u.), and intensities should not be compared directly between Figures 3a and 3b. A better indicator of the absolute signal intensities in the two spectra can be inferred from each spectrum's S/N. As expected based on number density and polar ordering considerations, spectra from the more expanded, liquid-

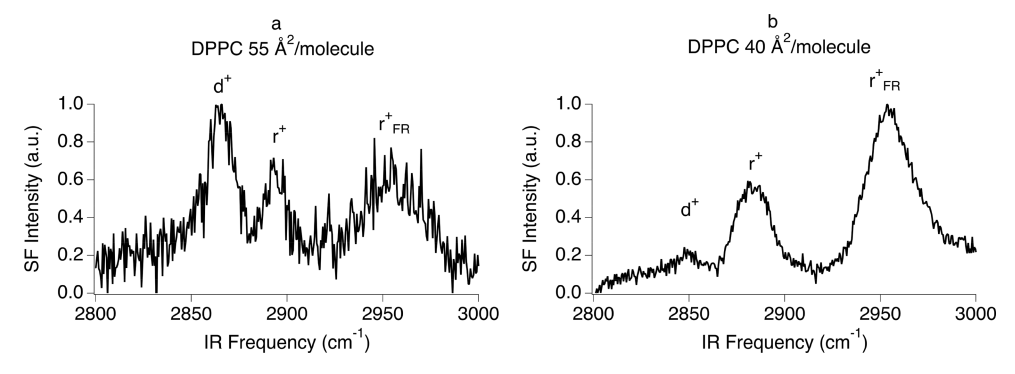


Figure 3. (a, left) VSFG spectra of 55 Å²/molecule DPPC on Millipore water at SSP polarization with peak assignments and an r^+/d^+ ratio of 0.60. (b, right). VSFG spectra of 40 Å²/molecule DPPC on Millipore water at SSP polarization with peak assignments and an r^+/d^+ ratio of 5.0.

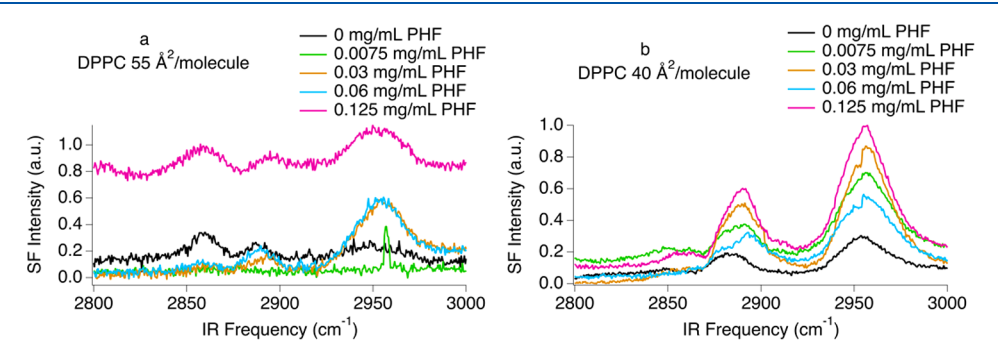


Figure 4. (a, left) VSFG spectra of 55 Å 2 /molecule DPPC on varying PHF/Millipore concentration subphase (all at SSP polarization), with an r^+ /d $^+$ ratio of 0.60 for 0 mg/mL PHF. (b, right). VSFG spectra of 40 Å 2 /molecule DPPC on varying PHF/Millipore concentration subphase (all at SSP polarization), with an r^+ /d $^+$ ratio of 5.0 for 0 mg/mL PHF.

condensed monolayer are weaker than those from tightly packed monolayers.

A ratio of the r⁺ and d⁺ intensities often serves as a sensitive indicator of alkyl chain conformational order.^{51–53} Under S_{sum}S_{vis}P_{IR} conditions, a well-ordered monolayer with alkyl chains in an all-trans conformation aligned predominantly along the surface normal will show a strong r⁺ band and a weak d⁺ band. The strong r⁺ results from the terminal methyl groups aligned with their local C_3 axes (and IR transition moments) directed in the laboratory z-axis. Two considerations lead to a weak d⁺ band in this well-ordered system: first, if the chains are all-trans and aligned along the surface normal, the CH₂ symmetric (and antisymmetric) IR transition moments will be aligned in-plane and will not be accessible to the SSP polarization combination, and second, an all-trans chain will have local inversion symmetry about each carbon-carbon bond, making the d⁺ transition symmetry forbidden in VSFG experiments. The introduction of gauche defects leads to more conformational disorder, a weaker r⁺, and the appearance of now-symmetry-allowed d+ transitions. Evidence of this behavior is readily apparent in Figures 3a and 3b, where the more loosely packed DPPC monolayer (55 Å²/molecule, Figure 3a) has an r^+/d^+ ratio of 0.6, and the tightly packed, well-ordered DPPC monolayer (40 Å²/molecule, Figure 3b) has an r^+/d^+ ratio of 5.0. This r^+/d^+ ratio will serve as an important indicator of how DPPC monolayers are affected by soluble PHFs. We note that the PHFs themselves have no VSFG active features in the region of interest (Figures S2 and S3). We also acknowledge that the r^+/d^+ ratio in the liquid condensed phase is very sensitive to small changes in surface coverage—r⁺/d⁺ ratios ranging from 0.4 to 1.4 for the liquid condensed phase can be attributed to this sensitivity.

Figures 4a and 4b show resonant VSFG spectra from DPPC monolayers at 55 and 40 Å²/molecule as a function of solution phase PHF concentration. Of importance is the scale of SF intensity. Although the data in Figures 4a and 4b are baseline corrected relative to a pure water-air interface, addition of PHF to the aqueous solution leads to a baseline that rises with increasing PHF concentration (also prevalent in Figures S2 and S3). Analysis of reflectivity data (Figure S1) shows that the surface reflectivity remains constant for all PHF concentrations tested in this work—the rising baseline is not attributed to a change in reflectivity. We speculate that the rising baseline may result either from changing surface charges or from broadband fluorescence emission following two-photon absorption, but these hypotheses are yet to be tested. The symmetric VSFG line shapes show that the increasing baseline signal is not coherent and thus does not interfere with the nonlinear VSFG response.

Changes in the VSFG spectra as a function of PHF concentration show that these soluble carbon particulates appreciably affect DPPC monolayer structure. These changes are most evident when comparing the r^+/d^+ intensity ratios from the different spectra. Figure 5 shows r^+/d^+ ratios for DPPC monolayers as a function of PHF concentration. These ratios were calculated from spectra acquired with an $S_{\text{sum}}S_{\text{vis}}P_{\text{IR}}$ polarization combination meaning that larger r^+/d^+ ratios reflect DPPC chains having more upright, *all-trans* conformations. Figure 5 suggests that PHFs at very low concentrations increase DPPC acyl chain ordering in a liquid condensed film more so than in a tightly packed film. We also note that in solutions having low PHF concentrations we frequently observed a high degree of variability in spectral intensities and line positions, even for systems that were

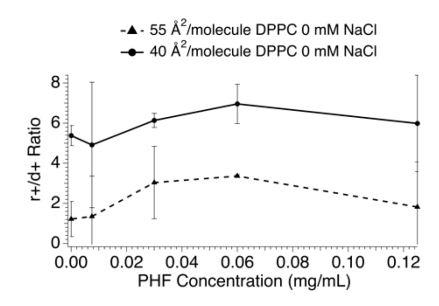


Figure 5. VSFG r^+/d^+ intensity ratios for DPPC on different concentrations of PHFs in neat Millipore at 55 and 40 Ų/molecule. The reported ratios represent the average of 3–6 independent experiments. The reported uncertainties represent the standard deviation of intensity ratios.

compositionally equivalent. This variability is reflected in some of the large uncertainties reported in Figure 5 and is also apparent in some of the spectra shown in Figure 4. Given the consistency observed in DPPC spectra in the absence of PHFs and in DPPC spetra at high PHF cocentrations, we interpret this variability with a dynamic equilibrium between the PHF solutes in bulk solution and the cooperatively adsorbed PHFs causing large fluctuations in DPPC organization.

This r⁺/d⁺ ratio behavior is consistent with results from Langmuir trough compression isotherms shown in Figure 1 assuming a cooperative adsorption mechanism that draws PHFs from solution to the DPPC covered water-air interface. In this scenario, PHFs are drawn to the surface by the DPPC monolayer and occupy the interstitial space between the DPPC monomers/islands in their liquid condensed state. When adsorbing to the surface, PHF solutes force the DPPC monomers into a smaller area, leading to greater conformational order (and higher surface pressures at a given MMA). For the tightly packed monolayer, the effects of PHF adsorption are less pronounced. Our overall assessment of these data is that, not surprisingly, the more tightly packed DPPC monolayer is consistently more ordered than the more loosely packed monolayer and that very low concentrations of PHF in bulk solution have pronounced effects on DPPC monolayer organization at both coverages. This assessment is most evident when comparing the tightly and loosely packed monolayers on a 0.06 mg/mL PHF solution, specifically with their respective spectra on solutions containing nothing but Millipore water.

We note that the reported uncertainties for the r^+/d^+ ratios can be large, especially at lower PHF concentrations. These uncertainties reflect large variability in intensity ratios from spectrum to spectrum and are likely the result of large fluctuations or—equivalently—a rapidly changing system. We attribute these fluctuations (at low PHF concentrations) to a dynamic equilibrium between PHF monomers and aggregates adsorbing to the interface, ultimately changing the interfacial composition and destabilizing DPPC monolayer structure. Alternatively, PHF adsorption to the interface at low PHF bulk concentrations might also be leading to changes in DPPC organization, ultimately leading to transient domains having either more or less order. Regardless of the origin of these large r⁺/d⁺ ratio uncertainties at low PHF concentrations, the magnitudes of these uncertainties are real and reproducible and further emphasize the importance of cooperative adsorption drawing PHF solutes to the surface in a way that significantly impacts lipid monolayer structure. Preliminary measurements (not shown) imply that these systems become much more stable when solution phase ionic strength increases.

Spectroscopic Ellipsometry (SE). SE experiments were performed to assess changes in the surface's optical properties and monolayer film thickness. Figure 6 shows calculated

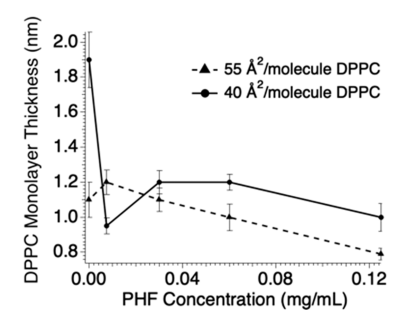


Figure 6. DPPC monolayer thickness on different concentrations of PHFs in neat Millipore water at 55 and 40 Å²/molecule. The reported monolayer thicknesses represent the average of six independent experiments. The reported uncertainties represent the standard deviation of the six thickness measurements for each concentration and range between ± 0.034 and ± 0.16 nm.

monolayer thickness of both the 55 and 40 ${
m \AA}^2$ DPPC monolayers as a function of PHF bulk solution concentration. The procedure for calculating film thicknesses is described in the Methods section and has been detailed in other reports. $^{54-56}$

SE data show that small amounts of PHF in the subphase lead to systematic changes in DPPC monolayer thickness. We note that because SE measurements of aqueous solutions containing only PHFs (e.g., samples whose surface tensions are reported in Figure 1) do not show reliable evidence of changing surface composition/thickness, the data reported in Figure 6 assume a model equivalent to that used to fit the DPPC-only monolayers on Millipore water. With the primary focus of this work being how the addition of PHFs changes DPPC structure and organization, this assumption allows us to observe direct changes to only DPPC with the inclusion of PHFs.

In Figure 6, the most extreme effects are observed for the 40 $Å^2$ /molecule monolayer. In the absence of PHF in solution, the tightly packed monolayer is 1.9 nm thick, a value consistent with previous reports. 54-56 An unappreciable amount (0.0075 mg/mL) of PHF in solution, however, leads to a 2-fold drop in monolayer thickness (0.95 \pm 0.05 nm). Changes in DPPC monolayer thickness are less pronounced at higher PHF concentrations, falling between 1.2 and 1.0 nm at concentrations up to 0.12 mg/mL. For the 55 Å²/molecule films, monolayer thickness is 1.1 nm in the absence of PHF, consistent with a "thinner", more disorganized monolayer and the correspondingly smaller r⁺/d⁺ ratio observed in the VSFG data (Figure 5). Monolayer thickness rises slightly at the lowest PHF concentration (to 1.2 nm) before falling monotonically to 0.8 at a PHF concentration of 0.12 mg/mL. When comparing trends in Figures 5 and 6, we propose that if PHF adsorption leads to an overall tilting of the monolayer structure, then the DPPC acyl chains could still retain their high degree of conformational order (with a small d+ and a smaller r+ as the IR transition moment is deflected away from surface normal), while the apparent monolayer width shrinks.

DISCUSSION

The studies described above were premised on the notion that interactions between soluble carbon nanoparticles and insoluble lipid monolayers change monolayer properties. Unknown when the work began was the concentration range where these interactions would be most pronounced. In this section, findings from each type of measurement—surface tension, VSFG, and SE—are summarized and interpreted in the context of the original hypothesis.

Surface Tension. Surface tension measurements resulted in two important discoveries. First, PHFs themselves are weakly surface active, creating terminal monolayer coverages of 7.5×10^{13} molecules/cm² at the water—air interface when bulk PHF concentrations approach 0.5 mg/mL. Fitting the data in Figure 1 results in a ΔG_{ads} for PHFs to the neat water-air interface of -30 ± 5 kJ/mol, a value of similar magnitude as for other nonionic surfactants such as Triton X-100.⁵⁷ Second, although PHFs are not strongly drawn to the water-air interface, their presence in solution has readily observable effects on DPPC monolayer compression isotherms which suggest a cooperative adsorption mechanism. Specifically, even at the lowest PHF bulk concentration tested in this work (0.0075 mg/mL) where surface coverages at the neat waterair interface are only 3×10^{12} molecules/cm², or ~4% of full monolayer coverage, PHFs cause the DPPC isotherm to shift to larger areas with consistently larger DPPC MMAs relative to DPPC on a pure water subphase. While this effect is often interpreted in terms of more expanded monolayers, an alternative explanation—especially in the context of one component being highly soluble in the subphase—is that cooperative interactions between the soluble PHF and insoluble DPPC draw the soluble PHF from solution, enriching interfacial organic composition and forcing the DPPC monomers into more tightly packed, better organized structures. Data from VSFG and spectroscopic ellipsometry measurements support this interpretation for the liquid condensed monolayer. For the tightly packed monolayer, interpretation of the optical data is more nuanced.

VSFG. To test the effects of PHF concentration on DPPC monolayer structure and organization, VSFG measurements were performed at two different DPPC surface coverages: 55 Å²/molecule (where the DPPC monolayer is in its liquid condensed state) and 40 Å²/molecule (corresponding to a tightly packed DPPC monolayer). As a measure of organization within the DPPC monolayer, a ratio of r⁺/d⁺ intensities was used, where a larger r⁺/d⁺ ratio corresponds to acyl chains that are tightly packed and vertically aligned, having very few gauche defects. Not surprisingly, the tightly packed monolayer on a pure aqueous subphase is much more ordered than the liquid condensed monolayer, with the two systems having average r^+/d^+ ratios of \sim 5.5 and \sim 1.0, respectively. With increasing PHF concentration, the r+/d+ ratio for the liquid condensed monolayer rises by a factor of 3 (to 3.0). Together with the surface tension data, these observations strongly suggest that PHFs are adsorbing to the surface, effectively compressing the liquid condensed DPPC monolayer, leading to higher surface pressures at a given DPPC MMA, and leading to more highly ordered DPPC monomers as described above.

SE. PHF-induced changes in tightly packed DPPC monolayer organization are more difficult to interpret. The well-ordered monolayer inferred from a large r^+/d^+ ratio

diminishes slightly with the addition of unappreciable amounts of PHF in solution (0.0075 mg/mL). This change in r^+/d^+ character coincides with a significant drop in monolayer thickness as measured by spectroscopic ellipsometry. Given that these experiments are performed independently and the results reproduce with equivalent samples, we believe these effects are real and coupled. Higher PHF concentrations—although still well below PHF concentrations that result in terminal monolayer coverage—lead at first to modest increases in r^+/d^+ and monolayer thickness (at a PHF concentration of 0.06 mg/mL) before both measures of DPPC film structure diminish at a PHF concentration of 0.125 mg/mL.

Reconciling a modest r⁺/d⁺ reduction and a 50% loss in film thickness at the lowest PHF concentration is challenging. The DPPC monolayer starts out tightly packed, so unlike with the liquid condensed system, no interstitial space at the water-air interface exists to accommodate adsorbing PHF monomers. If, however, PHF adsorption leads to an overall tilting of the monolayer structure, then the DPPC acyl chains could still retain their high degree of conformational order (with a small d+ and a smaller r+ as the IR transition moment is deflected away from surface normal), while the apparent monolayer width shrinks. The tilt would have to be extreme with a 50% loss of monolayer thickness corresponding to a 60° deflection from surface normal. Then, as more PHFs adsorb (from solutions having concentrations of 0.03 and 0.06 mg/mL), the effects induced by the initially adsorbed PHFs are diminished, and the chains adopt a more upright structure—the monolayer appears slightly thicker.

This interpretation is admittedly speculative, but it is consistent with the observations made from tightly packed DPPC monolayer on a PHF-containing subphase. We note that an alternative explanation for the dramatic thinning of the lipid monolayer could also result if a certain distribution of the lipids were in some way solubilized by PHF solutes. Loss of DPPC from the interface would consequently mean a larger mean molecular area and a correspondingly thinner monolayer film (similar to data from the 55 $Å^2$ /molecule system). Finally, we note that the SE models used to fit the data do not account for any effect that cooperatively adsorbed PHFs may have on the system—the models used strictly observe thickness changes to DPPC. This choice is intentional given that experiments have no way to quantify the amount of PHFs cooperatively adsorbed to the lipid film. Although PHFs themselves are weakly surface-active, ellipsometry experiments on the PHF/aqueous system (with no DPPC) were unable to distinguish between pure Millipore water and Millipore water with dissolved PHFs (with concentrations ranging from 0.0075 to 0.5 mg/mL). While the specific mechanisms responsible for these findings remain uncertain, what is clear is that highly soluble PHF solutes do cooperatively adsorb to tightly packed DPPC monolayers and that the effects of cooperative adsorption are significant even at the unappreciable PHF concentrations sampled in this work.

CONCLUSIONS

Results reported here use optical and thermodynamic techniques to examine the effects of PHFs, a model for aged BC, on DPPC monolayer properties. Initial studies focus on model systems having well-controlled lipid compositions as a function of PHF concentration to determine the mechanism(s) responsible for carbon particulate accumulation at the water—air interface. Surface tension, VSFG, and SE experiments all

show that soluble PHFs are drawn to the lipid-covered water air interface through a cooperative adsorption mechanism and that this effect is observable at extremely low PHF concentrations. For DPPC monolayers in their liquid condensed state where free surface area still exists between monomers, PHF adsorption (from bulk solution) effectively compresses the lipid monolayer, leading to more ordered acyl chains. For tightly packed DPPC monolayers, surface tension data, VSFG spectra, and spectroscopic ellipsometry measurements all show evidence of cooperative adsorption, although the data are more difficult to interpret. One possible interpretation is that the minute amount of PHFs cooperatively adsorbed to the tightly packed DPPC monolayer induce a net "tilting" of the monolayer away from surface normal, leading to a monolayer that appears less well-ordered (according to the r⁺/d⁺ order parameter) and simultaneously thinner. From a physiological perspective, results presented in this work suggest that carbon particulates, especially those on the smaller end of the PM_{2.5} range as approximated by the PHFs used here, may be enriched at the alveoli water-air interface rather than dissolving into the alveoli's water subphase.

ASSOCIATED CONTENT

Supporting Information

The Supporting Information is available free of charge at https://pubs.acs.org/doi/10.1021/acs.jpcb.2c02526.

Surface activity information about PHFs in Millipore, the effects that dissolved PHFs have on reflectivity at the air—water interface, and vibrational spectra of PHFs (PDF)

AUTHOR INFORMATION

Corresponding Author

Robert A. Walker — Chemistry and Biochemistry Department, Montana State University, Bozeman, Montana 59717, United States; Montana Materials Science Program, Montana State University, Bozeman, Montana 59717, United States; orcid.org/0000-0002-0754-6298; Phone: +1 (406) 994-7928; Email: rawalker@montana.edu

Authors

Nida Shaikh — Chemistry and Biochemistry Department, Montana State University, Bozeman, Montana 59717, United States; oorcid.org/0000-0003-4533-2116

Jessica M. Andriolo — Mechanical Engineering Department, Montana Technological University, Butte, Montana U.S. 59701, United States; Montana Tech Nanotechnology Laboratory, Montana Technological University, Butte, Montana 59701, United States; ⊚ orcid.org/0000-0002-0381-9076

Jack L. Skinner — Mechanical Engineering Department, Montana Technological University, Butte, Montana U.S. 59701, United States; Montana Tech Nanotechnology Laboratory and Materials Science Ph.D. Program, Montana Technological University, Butte, Montana 59701, United States

Complete contact information is available at: https://pubs.acs.org/10.1021/acs.jpcb.2c02526

Notes

The authors declare no competing financial interest.

ACKNOWLEDGMENTS

This material is based upon the work supported in part by the National Science Foundation EPSCoR Cooperative Agreement OIA-1757351. Any opinions, findings, and conclusions or recommendations expressed in this material are those of the author(s) and do not necessarily reflect the views of the National Science Foundation. The authors thank Dr. James Hilfiker and Dr. Jianing Sun from J.A. Woollam for assistance with spectroscopic ellipsometry measurements and for helpful discussions with data interpretation. The authors thank Dr. Samuel Bernhard from Montana State University for assistance with size exclusion chromatography (SEC)—HPLC measurements used to determine average number of hydroxyl groups for PHFs ($C_{60}(OH)_n$, mH_2O , where $n=22\pm 2$).

REFERENCES

- (1) Long, C. M.; Nascarella, M. A.; Valberg, P. A. Carbon black vs. Black carbon and other airborne materials containing elemental carbon: Physical and chemical distinctions. *Environ. Pollut.* **2013**, *181*, 271–86.
- (2) Sheridan, A. J.; Slater, J. M.; Arnold, T.; Campbell, R. A.; Thompson, K. C. Changes to dppc domain structure in the presence of carbon nanoparticles. *Langmuir* **2017**, *33*, 10374–10384.
- (3) Guzmán, E.; Santini, E.; Zabiegaj, D.; Ferrari, M.; Liggieri, L.; Ravera, F. Interaction of carbon black particles and dipalmitoylphosphatidylcholine at the water/air interface: Thermodynamics and rheology. *J. Phys. Chem. C* **2015**, *119*, 26937–26947.
- (4) Janssen, N. A.; Hoek, G.; Simic-Lawson, M.; Fischer, P.; van Bree, L.; ten Brink, H.; Keuken, M.; Atkinson, R. W.; Anderson, H. R.; Brunekreef, B.; et al. Black carbon as an additional indicator of the adverse health effects of airborne particles compared with pm10 and pm2.5. *Environ. Health Perspect.* **2011**, *119*, 1691–9.
- (5) Guzmán, E.; Liggieri, L.; Santini, E.; Ferrari, M.; Ravera, F. Effect of hydrophilic and hydrophobic nanoparticles on the surface pressure response of dppc monolayers. *J. Phys. Chem. C* **2011**, *115*, 21715—21722
- (6) Guzmán, E.; Santini, E.; Ferrari, M.; Liggieri, L.; Ravera, F. Interfacial properties of mixed dppc-hydrophobic fumed silica nanoparticle layers. *J. Phys. Chem. C* **2015**, *119*, 21024–21034.
- (7) Kokubo, K.; Matsubayashi, K.; Tategaki, H.; Takada, H.; Oshima, T. Facile synthesis of highly water-soluble fullerenes more than half-covered by hydroxyl groups. ACS Nano 2008, 2, 327–333.
- (8) Semenov, K. N.; Charykov, N. A.; Keskinov, V. N. Fullerenol synthesis and identification. Properties of the fullerenol water solutions. *J. Chem. Eng. Data* **2011**, *56*, 230–239.
- (9) Nandy, L.; Yao, Y.; Zheng, Z. H.; Riemer, N. Water uptake and optical properties of mixed organic-inorganic particles. *Aerosol Sci. Technol.* **2021**, *55*, 1398–1413.
- (10) Rastogi, N.; Satish, R.; Singh, A.; Kumar, V.; Thamban, N.; Lalchandani, V.; Shukla, A.; Vats, P.; Tripathi, S. N.; Ganguly, D.; et al. Diurnal variability in the spectral characteristics and sources of water-soluble brown carbon aerosols over delhi. *Sci. Total Environ.* **2021**, 794, 148589.
- (11) Textor, C.; Schulz, M.; Guibert, S.; Kinne, S.; Balkanski, Y.; Bauer, S.; Berntsen, T.; Berglen, T.; Boucher, O.; Chin, M.; et al. Analysis and quantification of the diversities of aerosol life cycles within aerocom. *Atmos. Chem. Phys.* **2006**, *6*, 1777–1813.
- (12) He, C.; Liou, K.-N.; Takano, Y.; Zhang, R.; Levy Zamora, M.; Yang, P.; Li, Q.; Leung, L. R. Variation of the radiative properties during black carbon aging: Theoretical and experimental intercomparison. *Atmos. Chem. Phys.* **2015**, *15*, 11967–11980.
- (13) Lary, D. J.; Shallcross, D. E.; Toumi, R. Carbonaceous aerosols and their potential role in atmospheric chemistry. *J. Geophys. Res.:* Atmos. 1999, 104, 15929–15940.
- (14) Wang, Y.; Ma, P. L.; Peng, J.; Zhang, R.; Jiang, J. H.; Easter, R. C.; Yung, Y. L. Constraining aging processes of black carbon in the

- community atmosphere model using environmental chamber measurements. J. Adv. Model. Earth Syst. 2018, 10, 2514-2526.
- (15) Harrod, K. S.; Jaramillo, R. J.; Rosenberger, C. L.; Wang, S.-Z.; Berger, J. A.; McDonald, J. D.; Reed, M. D. Increased susceptibility to RSV infection by exposure to inhaled diesel engine emissions. *Am. J. Respir. Cell Mol. Biol.* **2003**, 28, 451–463.
- (16) Borm, P. J.; Cakmak, G.; Jermann, E.; Weishaupt, C.; Kempers, P.; van Schooten, F. J.; Oberdorster, G.; Schins, R. P. Formation of pah-DNA adducts after in vivo and vitro exposure of rats and lung cells to different commercial carbon blacks. *Toxicol. Appl. Pharmacol.* **2005**, 205, 157–167.
- (17) Wang, T.; Xu, H.; Zhu, Y.; Sun, X.; Chen, J.; Liu, B.; Zhao, Q.; Zhang, Y.; Liu, L.; Fang, J.; et al. Traffic-related air pollution associated pulmonary pathophysiologic changes and cardiac injury in elderly patients with copd. *J. Hazard. Mater.* **2022**, *424*, 127463.
- (18) Kendall, M.; Brown, L.; Trought, K. Molecular adsorption at particle surfaces: A pm toxicity mediation mechanism. *Inhal. Toxicol.* **2004**, *16*, 99–105.
- (19) Levy, L.; Chaudhuri, I. S.; Krueger, N.; McCunney, R. J. Does carbon black disaggregate in lung fluid? A critical assessment. *Chem. Res. Toxicol.* **2012**, *25*, 2001–6.
- (20) Kunzi, L.; Krapf, M.; Daher, N.; Dommen, J.; Jeannet, N.; Schneider, S.; Platt, S.; Slowik, J. G.; Baumlin, N.; Salathe, M.; et al. Toxicity of aged gasoline exhaust particles to normal and diseased airway epithelia. *Sci. Rep.* **2015**, *5*, 11801.
- (21) Guzman, E.; Santini, E.; Zabiegaj, D.; Ferrari, M.; Liggieri, L.; Ravera, F. Interaction of carbon black particles and dipalmitoylphosphatidylcholine at the water/air interface: Thermodynamics and rheology. *J. Phys. Chem. C* **2015**, *119*, 26937–26947.
- (22) Arick, D. Q.; Choi, Y. H.; Kim, H. C.; Won, Y. Y. Effects of nanoparticles on the mechanical functioning of the lung. *Adv. Colloid Interface Sci.* **2015**, 225, 218–28.
- (23) Bernhard, W. Lung surfactant: Function and composition in the context of development and respiratory physiology. *Ann. Anat.* **2016**, 208, 146–150.
- (24) Link, K. A.; Hsieh, C.; Tuladhar, A.; Chase, Z.; Wang, Z.; Wang, H.; Walker, R. A. Vibrational studies of saccharide-induced lipid film reorganization at aqueous/air interfaces. *Chem. Phys.* **2018**, *512*, 104–110.
- (25) Ma, G.; Allen, H. C. New insights into lung surfactant monolayers using vibrational sum frequency generation spectroscopy. *Photochem. Photobiol.* **2006**, 82, 1517–1529.
- (26) Nag, K.; Perez-Gil, J.; Ruano, M. L. F.; Worthman, L. A. D.; Stewart, J.; Casals, C.; Keough, K. M. W. Phase transitions in films of lung surfactant at the air-water interface. *Biophys. J.* **1998**, *74*, 2983—2995.
- (27) Zhang, H.; Fan, Q.; Wang, Y. E.; Neal, C. R.; Zuo, Y. Y. Comparative study of clinical pulmonary surfactants using atomic force microscopy. *Biochim. Biophys. Acta* **2011**, *1808*, 1832–1842.
- (28) Ma, G.; Allen, H. C. Dppc langmuir monolayer at the air-water interface: Probing the tail and head groups by vibrational sum frequency generation spectroscopy. *Langmuir* **2006**, 22, 5341–5349.
- (29) Plant, A. L. Supported hybrid bilayer membranes as rugged cell membrane mimics. *Langmuir* **1999**, *15*, 5128–5135.
- (30) Sackmann, E. Supported membranes: Scientific and practical applications. *Science* **1996**, *271*, 43–48.
- (31) Perring, A. E.; Schwarz, J. P.; Markovic, M. Z.; Fahey, D. W.; Jiminez, J. L.; Campuzano-Jost, P.; Palm, B. D.; Wisthaler, A.; Mikoviny, T.; Diskin, G.; et al. In situ measurements of water uptake by black carbon-containing aerosol in wildfire plumes. *J. Geophys. Res. Atmos.* 2017, 122, 1086–1097.
- (32) Metcalf, A. R.; Loza, C. L.; Coggon, M. M.; Craven, J. S.; Jonsson, H. H.; Flagan, R. C.; Seinfeld, J. H. Secondary organic aerosol coating formation and evaporation: Chamber studies using black carbon seed aerosol and the single-particle soot photometer. *Aerosol Sci. Technol.* **2013**, *47*, 326–347.
- (33) Moteki, N.; Kondo, Y. Dependence of laser-induced incandescence on physical properties of black carbon aerosols:

- Measurements and theoretical interpretation. *Aerosol Sci. Technol.* **2010**, 44, 663–675.
- (34) Schmitt, C. G.; All, J. D.; Schwarz, J. P.; Arnott, W. P.; Cole, R. J.; Lapham, E.; Celestian, A. Measurements of light-absorbing particles on the glaciers in the cordillera blanca, peru. *Cryosphere* **2015**, *9*, 331–340.
- (35) Link, K. A.; Spurzem, G. N.; Tuladhar, A.; Chase, Z.; Wang, Z.; Wang, H.; Walker, R. A. Organic enrichment at aqueous interfaces: Cooperative adsorption of glucuronic acid to dppc monolayers studied with vibrational sum frequency generation. *J. Phys. Chem. A* **2019**, *123*, 5621–5632.
- (36) Link, K. A.; Spurzem, G. N.; Tuladhar, A.; Chase, Z.; Wang, Z.; Wang, H.; Walker, R. A. Cooperative adsorption of trehalose to dppc monolayers at the water-air interface studied with vibrational sum frequency generation. *J. Phys. Chem. B* **2019**, *123*, 8931–8938.
- (37) Rosen, M. J. Surfactants and Interfacial Phenomena, 3rd ed.; John Wiley & Sons, Inc.: Hoboken, NJ, 2004; pp 49-64.
- (38) Gzyl-Malcher, B.; Paluch, M. Studies of lipid interactions in mixed langmuir monolayers. *Thin Solid Films* **2008**, *516*, 8865–8872.
- (39) Blume, A. Lipids at the air water interface. *ChemTexts* **2018**, *4*, 3.
- (40) Shen, Y. R. Surface properties probed by second-harmonic and sum-frequency generation. *Nature* **1989**, 337, 519–525.
- (41) Shen, Y. R.; Ostroverkhov, V. Sum-frequency vibrational spectroscopy on water interfaces: Polar orientation of water molecules at interfaces. *Chem. Rev.* **2006**, *106*, 1140–1154.
- (42) Rangwalla, H.; Dhinojwala, A. Probing hidden polymeric interfaces using ir-visible sum-frequency generation spectroscopy. *J. Adhes.* **2004**, *80*, 37–59.
- (43) Noskov, B. A.; Timoshen, K. A.; Akentiev, A. V.; Chirkov, N. S.; Dubovsky, I. M.; Lebedev, V. T.; Lin, S. Y.; Loglio, G.; Miller, R.; Sedov, V. P.; et al. Dynamic durface properties of fullerenol solutions. *Langmuir* **2019**, *35*, 3773–3779.
- (44) Liu, W.-J.; Jeng, U.; Lin, T.-L.; Lai, S.-H.; Shih, M. C.; Tsao, C.-S.; Wang, L. Y.; Chiang, L. Y.; Sung, L. P. Adsorption of dodecahydroxylated-fullerene monolayers at the air-water interface. *Phys. B (Amsterdam, Neth.)* **2000**, 283, 49–52.
- (45) Akentiev, A. V.; Gorniaia, S. B.; Isakov, N. A.; Lebedev, V. T.; Milyaeva, O.; Sedov, V. P.; Semenov, K. N.; Timoshen, K. A.; Noskov, B. A. Surface properties of fullerenol c60(oh)20 solutions. *J. Mol. Liq.* **2020**, *306*, 112904.
- (46) Wielgus, A. R.; Zhao, B.; Chignell, C. F.; Hu, D. N.; Roberts, J. E. Phototoxicity and cytotoxicity of fullerol in human retinal pigment epithelial cells. *Toxicol. Appl. Pharmacol.* **2010**, *242*, 79–90.
- (47) Can, S. Z.; Chang, C. F.; Walker, R. A. Spontaneous formation of dppc monolayers at aqueous/vapor interfaces and the impact of charged surfactants. *Biochim. Biophys. Acta* **2008**, *1778*, 2368–2377.
- (48) MacPhail, R. A.; Strauss, H. L.; Snyder, R. G.; Elliger, C. A. C-h stretching modes and the structure of n-alkyl chains. 2. Long, all-trans chains. *J. Phys. Chem.* **1984**, *88*, 334–341.
- (49) Snyder, R. G.; Strauss, H. L.; Elliger, C. A. C-h stretching modes and the structure of n-alkyl chains. 1. Long, disordered chains. *J. Phys. Chem.* **1982**, *86*, 5145–5150.
- (50) Richmond, G. L. Molecular bonding and interactions at aqueous surfaces as probed by vibrational sum frequency spectroscopy. *Chem. Rev.* **2002**, *102*, 2693–2724.
- (51) Can, S. Z.; Mago, D. D.; Esenturk, O.; Walker, R. A. Balancing hydrophobic and hydrophilic forces at the water/vapor interface: Surface structure of soluble alcohol monolayers. *J. Phys. Chem. C* **2007**, *111*, 8739–8748.
- (52) Ma, G.; Allen, H. C. Condensing effect of palmitic acid on dppc in mixed langmuir monolayers. *Langmuir* **2007**, 23, 589–597.
- (53) Walker, R. A.; Gragson, D. E.; Richmond, G. L. Induced changes in solvent structure by phospholipid monolayer formation at a liquid-liquid interface. *Colloids Surf., A* 1999, *154*, 175–185.
- (54) Yun, H.; Choi, Y.-W.; Kim, N.; Sohn, D. Physicochemical properties of phosphatidylcholine (pc) monolayers with different alkyl chains, at the air/water interface. *Bull. Korean Chem. Soc. B* **2003**, 24, 377–383.

- (55) Finot, E.; Markey, L.; Hane, F.; Amrein, M.; Leonenko, Z. Combined atomic force microscopy and spectroscopic ellipsometry applied to the analysis of lipid-protein thin films. *Colloids Surf., B* **2013**, *104*, 289–293.
- (56) Kamble, S.; Patil, S.; Kulkarni, M.; Murthy, A. V. R. Spectroscopic ellipsometry of fluid and gel phase lipid bilayers in hydrated conditions. *Colloids Surf., B* **2019**, *176*, 55–61.
- (57) Danov, K. D.; Kralchevsky, P. A. The standard free energy of surfactant adsorption at air/water and oil/water interfaces: Theoretical vs. Empirical approaches. *Colloid J.* **2012**, *74*, 172–185.

□ Recommended by ACS

Unusual Robustness of Neurotransmitter Vesicle Membranes against Serotonin-Induced Perturbations

Ankur Gupta, Sudipta Maiti, et al.

FEBRUARY 16, 2023

THE JOURNAL OF PHYSICAL CHEMISTRY B

READ 🗹

Pathways of Membrane Solubilization: A Structural Study of Model Lipid Vesicles Exposed to Classical Detergents

Victoria Ariel Bjørnestad and Reidar Lund

MARCH 09, 2023

LANGMUIR

READ 🗹

Orientation of Cholesterol in Polyunsaturated Lipid Bilayers

Iain M. Braithwaite and James H. Davis

DECEMBER 08, 2022

LANGMUIR

READ **C**

Recombination between 13 C and 2 H to Form Acetylide (13 C $_{2}$ H-) Probes Nanoscale Interactions in Lipid Bilayers via Dynamic Secondary Ion Mass Spectrometry: Cholester...

Dashiel S. Grusky, Steven G. Boxer, et al.

JUNE 27, 2022

ANALYTICAL CHEMISTRY

READ 🗹

Get More Suggestions >